

Electrode Reactions of Nd³⁺/Nd Couple in LiCl-KCl-NdCl₃ Solutions at Solid W and Liquid Cd Electrodes

Jee-Hyung Sim¹, Yong-Soo Kim^{1,*}, Seung-Woo Paek², Si-Hyung Kim², Sung-Jai Lee²

¹ Department of Nuclear Engineering, Hanyang University, 222, Wangsimni-ro, Seongdong-gu, Seoul, 04763, Republic of Korea

² Korea Atomic Energy Research Institute, 1045 Daedeok-daero, Yuseong-gu, Daejeon, 34057, Republic of Korea

*E-mail: yongskim@hanyang.ac.kr

Received: 24 November 2017 / Accepted: 8 January 2018 / Published: 5 February 2018

The behavior of Nd(III)/Nd(0) redox reaction at a solid tungsten (W) and liquid cadmium (Cd) electrodes in the LiCl-KCl-NdCl₃ system at 773 K was analyzed by using a cyclic voltammetry. The Nd(III)/Nd(0) reaction in the solid W electrode was found to occur in two steps through the process of Nd(II) ion generation. As the analytic results of the maximum current value according to scan rates in the region of 0.05 V/s to 0.3 V/s, the Nd(III)/Nd(II) reaction showed reversible reaction characteristics over the whole range, while the Nd(II)/Nd(0) reaction showed the reversible reaction in the region of 0.05 V/s to 0.2 V/s, as well as the quasi-reversible in the range of 0.2 V/s or higher. Furthermore, the diffusion coefficients of Nd(III) ion and Nd(II) ion were calculated by using the maximum current value, which were considerably consistent with the previous results of other researchers. The reduction potential of the Nd(III)/Nd(0) reaction in the liquid Cd electrode was measured as approximately 0.54 V higher than that of the solid W electrode because the reduced Nd formed an Nd-Cd intermetallic compound with a liquid Cd electrode, lowering the activity of Nd. To confirm this mechanism, experiments using Cd-coated W electrodes were conducted by using cyclic voltammetry and chronopotentiometry. The experimental results showed that 6 Nd-Cd intermetallic compounds were present. When the ratio of Cd is the highest, NdCd₁₁ is formed, and the potential in this case was very similar to the potential at the liquid Cd electrode. Furthermore, the Gibbs free energy and activity coefficient of Nd-Cd intermetallic compounds were calculated by analyzing the results of chronopotentiometry. The results could thermodynamically explain the potential difference of the Nd(III)/Nd(0) reactions occurring between the solid W electrode and the liquid Cd electrode.

Keywords: Electrochemical reaction, LiCl-KCl-NdCl₃ eutectic, Liquid cadmium cathode, Nd-Cd intermetallic compound

1. INTRODUCTION

Spent nuclear fuel discharged from a nuclear power plant contains a large number of radioactive isotopes, and has characteristics of high radioactivity and high exothermicity. Furthermore, studies have reported that the spent nuclear fuel contains a significant amount of actinide nuclides such as U and TRUs (transuranic elements), which can be used as valuable resources [1]. Thus, the management and handling of spent nuclear fuel is a crucial issue, and public attention on the issue has been growing recently. Numerous international studies have been conducted on pyroprocess, which is one of the promising option for treating spent nuclear fuel, as a technology for recovering actinide nuclides including U, and highly radioactive and long-half-life nuclides [2-5]. Pyroprocess can increase the utilization rate of uranium resources as well as the utilization efficiency of the repository, and the pyroprocess is further advantageous in that the TRUs are recovered simultaneously without separating the TRUs, thereby having resistance to nuclear proliferation. To achieve this goal, actinide and lanthanide nuclides are recovered by using electrochemical techniques using solid and liquid electrodes in the molten salt in the main steps of the pyroprocess [6, 7].

In this regard, U is recovered by using a solid electrode in the electrorefining process, and U and TRUs are simultaneously recovered by using a liquid electrode in the electrowinning process. The reason for such selection of different electrodes is due to a difference in the reduction potential between the nuclides according to the shape of the electrode [8]. While the separation of solid electrodes is easy because of the large difference in the reduction potential, the separation of liquid electrodes is not easy due to the small difference. Thus, the solid electrode is primarily used to recover the U highly contained in the spent nuclear fuel, and the liquid electrode is used to simultaneously recover the remaining U and TRUs. However, the liquid electrode simultaneously recovers RE (rare earth) nuclides, which are similar in electrochemical properties to TRU [9]. In this case, RE would be probably contained in the nuclear fuel of sodium cooled fast reactor (SFR) which is manufactured by using the pyroprocess product. Because RE has a high neutron absorption, lowering the neutron efficiency in the reactor, the amount of RE from the group recovery should be minimized [10, 11]. In this regard, it is crucial to understand the electrochemical behaviors and thermodynamic characteristics of reactions between various electrodes and materials such as U, TRUs, and REs to derive operating conditions and increase efficiency of pyroprocess.

Thus, various studies using electrochemical transient techniques have been conducted, reporting that the electrochemical transient techniques are a useful method for analyzing electrochemical and thermodynamic characteristics of electroactive materials in molten salt [12-16]. Particularly, cyclic voltammetry (CV) and potentiometry are useful methods to provide various information such as electrode potential, diffusion coefficient, activity coefficient, intermetallic compound formation and corresponding Gibbs free energy of electroactive materials [17-19]. By using the methods, various studies have been conducted on the reaction characteristics of solid electrodes and liquid Cd electrodes against various chlorides such as UCl_3 , PuCl_3 , NpCl_3 , LaCl_3 , CeCl_3 , and PrCl_3 in the LiCl-KCl molten salt system [10,20-25]. However, in the case of Nd, which has the highest ratio of RE in the spent fuel, several researchers provide meaning information such as the electrode potential and the diffusion coefficient for solid electrodes [11]. However, there are few studies on the

electrochemical properties and electrode reactions in liquid Cd electrodes. In particular, it is impossible to use TRU elements in South Korea due to the nuclear nonproliferation policy. Therefore, despite the fact that NdCl_3 is mainly used as a substitute in the experiment of pyroprocess, only a very limited reliable data was obtained by Kim et al. [25].

Thus, this study conducted the electrochemical experiment using NdCl_3 , to analyze the electrode reaction behavior in solid W electrode and liquid Cd electrode. Furthermore, the formation process of Nd_xCd_y intermetallic compound was analyzed by using a Cd-coated W electrode to thermodynamically analyze the potential difference between the solid electrode and the liquid Cd electrode. Also, thermodynamic properties are calculated by using the experimental results. Electrochemical techniques such as CV, chronopotentiometry (CP), square wave voltammetry (SWV) and differential pulse voltammetry (DPV) were used for this purpose.

2. EXPERIMENTAL

2.1 Chemicals

Anhydrous LiCl-KCl (99.99 % purity) with a composition ratio of 59:41 mol%, anhydrous NdCl_3 (99.99 % purity), anhydrous CdCl_2 (99.999 % purity), and Cd shot (99 % purity) were purchased from Sigma-Aldrich Co. Unlike the other three samples, the Cd shot was delivered in a non-vacuum packaged condition, which suggested that the surface was partially oxidized. Accordingly, the Cd shot was dissolved in a Pyrex tube to increase the purity of Cd. When the Cd shot was melted, yellowish cadmium oxide was observed on the surface, and by removing cadmium oxide, purer Cd was obtained.

2.2 Electrochemical apparatus and methods

Each electrochemical experiment was performed in a glove box with an Ar atmosphere in which the concentration of oxygen and moisture was maintained as 3 ppm or less. The electrochemical cell had a quartz tube with an inner diameter of 15 mm, and the temperature inside the electrochemical cell was maintained at 773 ± 1 K by using an external electric furnace. All experiments were performed by using a 3-electrode cell, and CV experiments were performed by using a solid W electrode and a liquid Cd electrode with a diameter of 0.8 mm as the working electrodes. In the experiment of liquid Cd electrode, Cd was dissolved at the bottom of the electrochemical cell first and then chlorides were charged to completely separate the two layers. A stainless-steel wire with a diameter of 1 mm was used as a lead wire. Glassy carbon with a diameter of 3 mm was used as a counter electrode. The electrode area was 0.256 cm^2 , 1.767 cm^2 , and 1.955 cm^2 for the W electrode, the liquid cadmium electrode, and the counter electrode, respectively. As the reference electrode, Ag/Ag^+ electrode containing a Ag wire in 1 mol% $\text{AgCl}/\text{LiCl-KCl}$ solution was used.

For the use of electrochemical techniques, the SP-240 Potentiostat from Biologic was used, and the data was acquired by using EC-Lab 10.44 version software.

3. RESULTS AND DISCUSSION

3.1 Electrochemical reaction of NdCl_3 in LiCl-KCl at W electrode

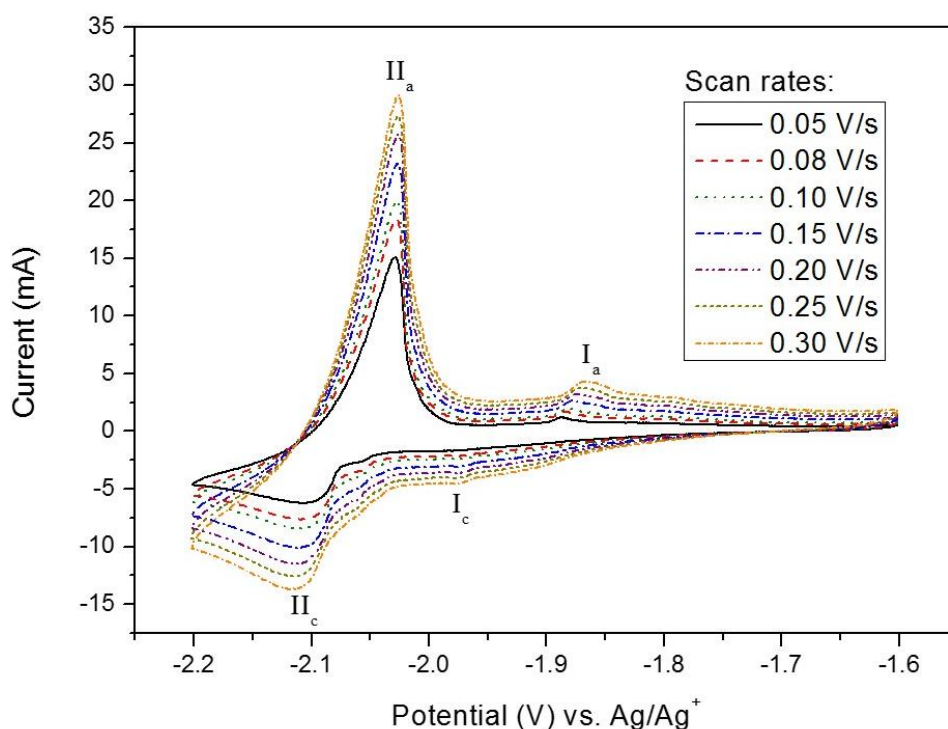
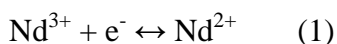


Figure 1. Cyclic voltammograms of LiCl-KCl-NdCl_3 at W electrode for different scan rates. Temperature: 773 K; Concentration of NdCl_3 : 1 wt%; Electrode area: 0.256 cm^2 .

The CV for $\text{LiCl-KCl-1 wt\% NdCl}_3$ at 773 K was measured by using an inactive W electrode. Fig. 1 shows the CV results measured at a scan rate of 0.05 V/s to 0.3 V/s, indicating that two reduction peaks and two oxidation peaks appeared on the CV curve. The results suggest that the redox reaction of NdCl_3 on the inactive W electrode takes place in two steps. The studies by Vandarkuzhali et al., Castrillejo et al., Masset et al., and Fukusawa et al. showed similar results in the experiments with the redox reaction of NdCl_3 on inactive electrodes [13, 14, 25, 26]. Those studies concluded that the Nd(III)/Nd(0) redox reaction proceeds through the intermediate process of Nd(II) ion generation, resulting in the two-step reaction takes place as described below.



Thus, the results suggest that the peaks I_c and I_a were obtained from the Nd(III)/Nd(II) reactions and the peaks II_c and II_a were obtained from the Nd(II)/Nd(0) reaction.

3.1.1 Analysis of peak I_c

Fig. 1 confirms that the oxidation peak potential formed between -1.8 V and -1.9 V, and the reduction peak potential for peak I formed between -1.9 V and -2.0 V, respectively. Particularly, as

shown in Fig. 2, the reduction peak potential is maintained as nearly constant despite the changes in the scan rate.

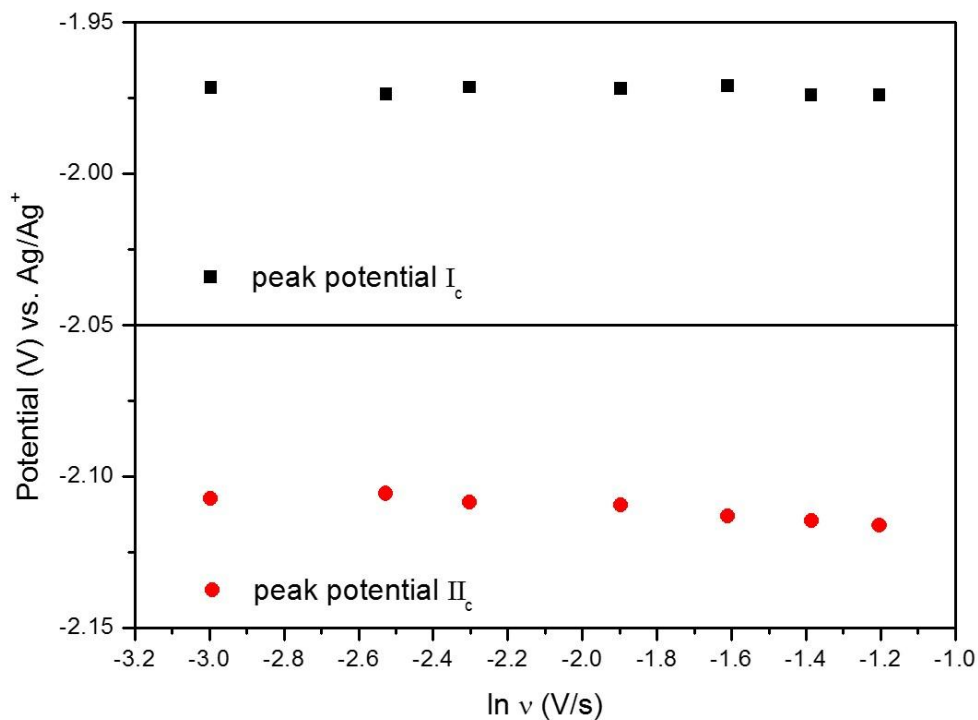


Figure 2. Plot of the cathodic peak potential as a function of logarithm of the scan rates at 773 K.

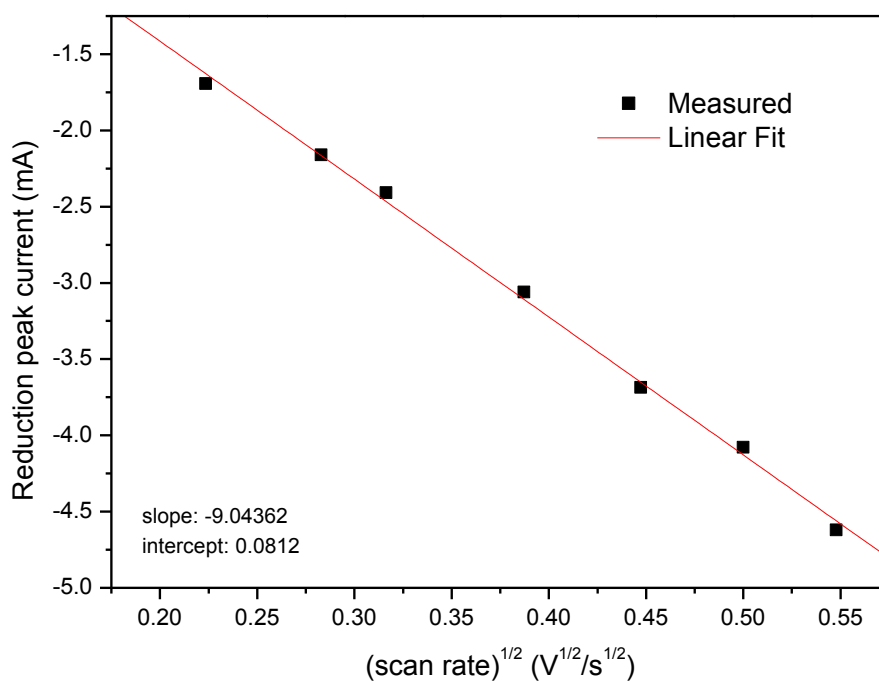


Figure 3. Plot of current for peak I_c vs. square root of scan rate for LiCl-KCl-1 wt% NdCl₃.

Furthermore, Fig. 3 confirmed that the reduction peak current is linearly proportional to the square root of the scan rate. These results indicate that the reaction process is reversible and further controlled by the diffusion of electroactive species.

In reversible electrochemical reactions involving soluble-soluble species, the following equation is satisfied between the difference between the peak potential (E_p) and the half peak potential ($E_{p/2}$), and the number of electrons participating in the reaction [27].

$$E_{p/2} - E_p = 2.2 \left(\frac{RT}{nF} \right) \quad (3)$$

where n is the number of electrons involved in the reaction, R is the gas constant (8.314 J/mol K), T is the absolute temperature (K), and F is the Faraday constant (C/mol).

Table 1 shows that n values are calculated according to the above Equation (3), and the values are close to 1 at all scan rates. Thus, I_c and I_a correspond to the Nd(III)/Nd(II) redox reaction, which suggests that this reaction is a reversible process controlled by diffusion. A study by Novoselova et al. further obtained the same results through an experiment using a linear sweep voltammetry method. According to the study, the reduction of Nd(III) ion in the LiCl-KCl-CsCl-NdCl₃ system takes place in two steps. The first step is the reversible reaction of Nd (III)/Nd (II) [28].

Table 1. Experimental and calculated data for the number of electrons transferred

V (Vs ⁻¹)	Peak I _c			Peak II _c		
	E _p (V)	E _{p/2} (V)	n	E _p (V)	E _{p/2} (V)	n
0.05	-1.9715	-1.8397	1.11	-2.1072	-2.0802	1.90
0.08	-1.9736	-1.8412	1.10	-2.1056	-2.0811	2.10
0.10	-1.9714	-1.8409	1.12	-2.1084	-2.0819	1.94
0.15	-1.9719	-1.8299	1.03	-2.1094	-2.0829	1.94
0.20	-1.9710	-1.8400	1.11	-2.1130	-2.0830	1.72
0.25	-1.9741	-1.8407	1.09	-2.1147	-2.0827	1.61
0.30	-1.9740	-1.8396	1.09	-2.1162	-2.0832	1.55

Accordingly, the diffusion coefficient of Nd(III) ion can be obtained by using the CV results. In the reduction reaction between the soluble-soluble species controlled by diffusion, the maximum current is represented by the Randles-Sevcik Equation [29].

$$i_{pc} = 0.446(nF)^{3/2}(RT)^{-1/2}ACD^{1/2}\nu^{1/2} \quad (4)$$

where A is the electrode area (cm²), C is the concentration of the electroactive substance (mol/cm³), D is the diffusion coefficient (cm²/s), and ν is the scan rate (V/s). Assuming that all the Nd

ions present in the LiCl-KCl-1 wt% NdCl₃ salt are Nd(III) ions, $D_{Nd(III)}$ is $0.71 \pm 0.04 \times 10^{-5} \text{ cm}^2/\text{s}$, which consistent with the experimental results of other researchers, as shown in Table 2.

Table 2. Diffusion coefficients of Nd ion in LiCl-KCl-1 wt% NdCl₃ at 773 K

	This study	Vandarkuzhali et al.[25]	Glatz et al. *[32]
$D_{Nd(III)}$ (cm ² /s)	$0.71 \pm 0.04 \times 10^{-5}$	$0.54 \pm 0.05 \times 10^{-5}$	0.95×10^{-5}
$D_{Nd(II)}$ (cm ² /s)	$1.98 \pm 0.07 \times 10^{-5}$	$1.69 \pm 0.05 \times 10^{-5}$	1.25×10^{-5}

* Glatz et al. performed at 733 K.

3.1.2 Analysis of peak II_c

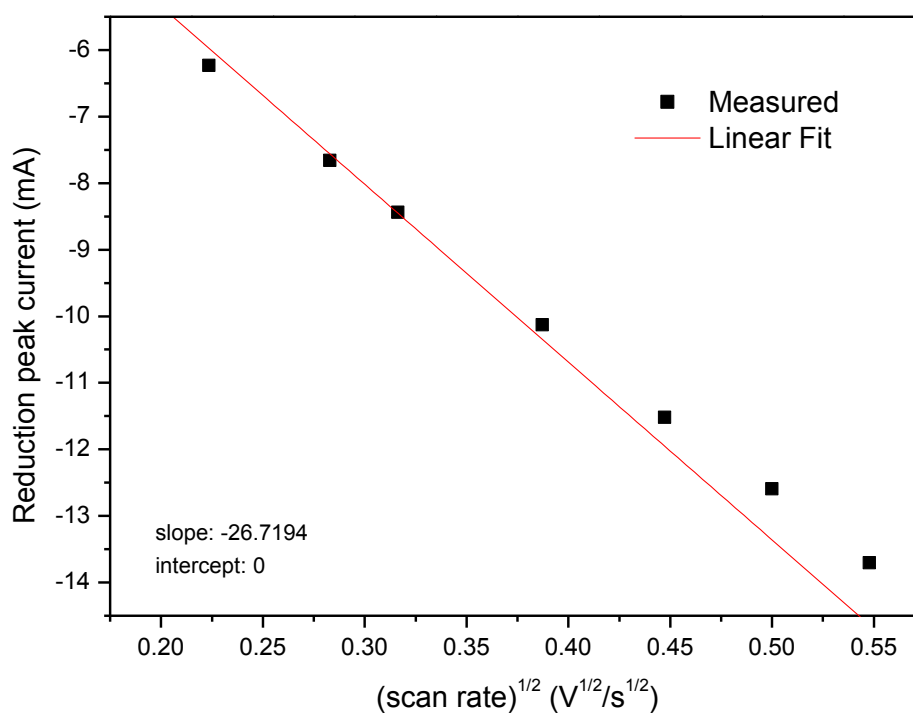


Figure 4. Plot of current for peak II_c vs. square root of scan rate for LiCl-KCl-1 wt% NdCl₃.

The reduction peak potential for Peak II tends to increase as the scan rate increases, unlike the peak (reduction peak) potential for peak I. Fig. 2 confirms that when the scan rate is 0.2 V/s or higher, the potential increases as the scan rate increases. The results confirm that while the reduction peak current is linearly proportional to the square root of the scan rate until the scan rate reaches 0.2 V/s, unlike the peak I, the trend is slightly deviating from the proportionality after the 0.2 V/s (Fig. 4). Thus, the results in this experiment suggest that the reduction reaction of Nd(II) ions occurred in different patterns before and after the point of 0.2 V/s scan rate. The reversible electrochemical reaction occurring between soluble-insoluble species satisfies the following Equation (5) between the

difference between the peak potential (E_p) and the half peak potential ($E_{p/2}$) and the number of electrons participating in the reaction [30].

$$E_{p/2} - E_p = 0.77 \left(\frac{RT}{nF} \right) \quad (5)$$

The calculation of the n values according to Equation (5) confirms that the n value is close to 2 before 0.2 V/s, while the n value gradually decreases from 0.2 V/s or higher (Table 1). These results indicate that Nd(II)/Nd(0) redox reaction reversibly occurs at the scan rate of 0.05 V/s to 0.2 V/s, and the redox reaction becomes quasi-reversible at 0.2 V/s or higher. A similar conclusion can be found in Vandarkuzhali et al. It also appears in experimental results. In the experiment using LiCl-KCl-NdCl₃, the study conducted the CV at a scan rate of 0.01 V/s to 0.25 V/s, and concluded that the Nd(II)/Nd(0) reaction was reversible in the range of 0.01 V/s to 0.05 V/s, and quasi-reversibly in the range of 0.075 V/s to 0.25 V/s [25]. On the other hand, a study by Fukasawa et al. performed the CV at a scan rate of 0.1 V/s and showed that the Nd(II)/Nd(0) reaction was reversible [26]. Thus, the overall results suggest that the scan rate has a significant influence on the Nd(II)/Nd(0) reaction according to the detailed experimental conditions and the configuration of the electrolytic cell.

Therefore, the diffusion coefficient can be obtained for the scan rate range of 0.05 V/s to 0.2 V/s in which the Nd(II)/Nd(0) reaction reversibly occurs. In the reversible reaction between the soluble-insoluble species, the maximum reduction current and the scan rate follow the Berzins-Delahay Equation [31].

$$i_{pc} = 0.61(nF)^{3/2}(RT)^{-1/2}ACD^{1/2}\nu^{1/2} \quad (6)$$

where C is the concentration of Nd(II) ion, and since Nd(II) ion is generated from Nd(III) ion, it is assumed that $C_{Nd(II)}=C_{Nd(III)}$. The same assumption was used in the studies by Vandarkuzhali et al., and Glatz et al. in the process of determining the diffusion coefficient of Nd(II) ions, while the study by Kuznetsov et al. showed that the assumption had no significant effect on the outcomes [25,32]. The study by Kuznetsov et al. conducted experiments using EuCl₂ and EuCl₃ to determine the diffusion coefficients of Eu(II) ions and Eu(III) ions, respectively. The results showed no significant difference from those with the assumption that $C_{Eu(II)}=C_{Eu(III)}$ [27]. The accordingly calculated $D_{Nd(II)}$ was $1.98 \pm 0.07 \times 10^{-5}$ cm²/s, which is highly consistent with the results of other researchers (Table 2).

3.2 Electrochemical reaction of NdCl₃ in LiCl-KCl at liquid Cd electrode

Fig. 5 shows a cyclic voltammogram measured at a scan rate of 0.05 V/s by using a liquid Cd electrode for pure LiCl-KCl and LiCl-KCl-1 wt% NdCl₃. Curves (a) and (b) represents the CV curve for LiCl-KCl-1 wt% NdCl₃ with pure LiCl-KCl, respectively. The curve (a) shows that the oxidation-reduction potential for Nd is not clearly distinguished from that for the solid W electrode because the oxidation potential and reduction potential of Li and Nd have no significant difference in the reaction with the liquid cathode.

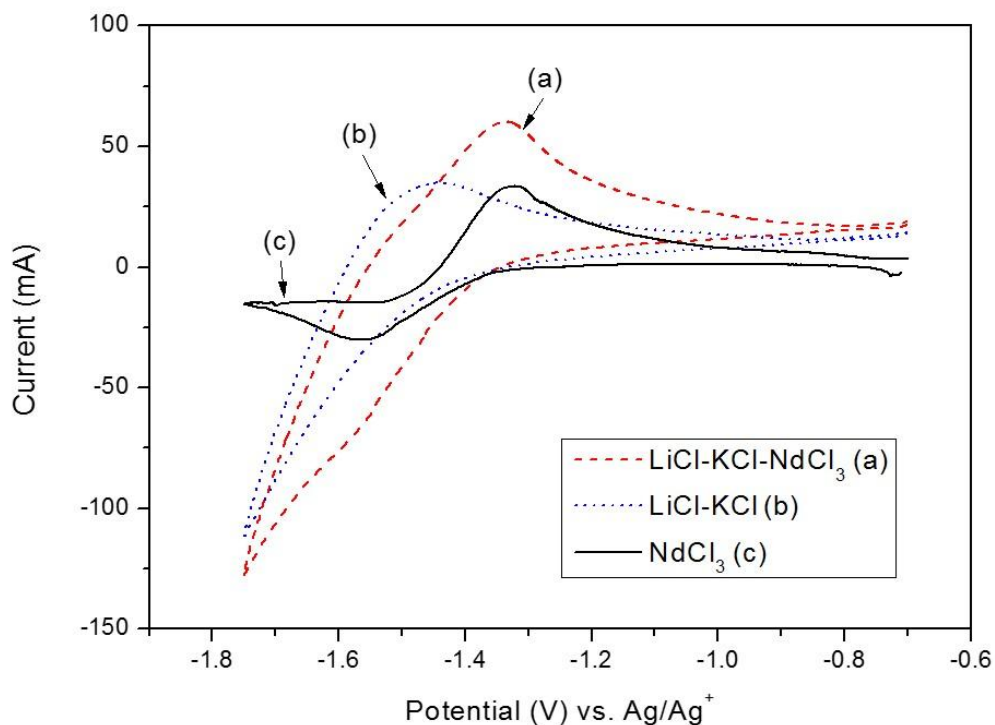


Figure 5. Cyclic voltammograms of LiCl-KCl-NdCl₃ at liquid Cd electrode with the scan rate of 0.05 V/s. Temperature: 773 K; Concentration of NdCl₃: 1 wt%; Electrode area: 1.767 cm²

Thus, the reduction current starts to increase between -1.3 V and -1.4 V in both curves, which shows no clear difference. However, as the potential increases negative direction, the current of the curve (a) increases more rapidly than that of the curve (b). The reason is that the reduction current of the curve (b) is due to the reduction of Li⁺ alone while the reduction current of the curve (a) is due to the simultaneous reduction of Li⁺ ions and Nd³⁺ ions. Accordingly, the difference between curve (a) and curve (b) is constructed to obtain a CV curve for NdCl₃ alone, which can remove the influence of the Li. The so obtained curve (c) shows a pair of oxidation-reduction peaks, which can be attributed to the Nd(III)/Nd(0) reaction, assuming no reaction or very weak reaction between Li and Nd. This method has been widely used by many researchers [10,18,33]. Thus, the results show the reduction peak potential and the oxidation peak potential of curve (c) as -1.568 V and -1.328 V, respectively.

The reduction peak potential is formed where approximately 0.54 V larger in the positive direction with respect to the potential at the solid W electrode. Many researchers have explained that the potential difference in the M⁺/M reaction exists because the activity coefficients of TRUs and REs, when reacted at the liquid electrode, are smaller than those at the solid electrode [34-36]. Accordingly, the activity can be thermodynamically calculated by using the potential difference that occurs in the process where the reduced metal reacts with the liquid Cd to form the M-Cd intermetallic compound. The potential between the reference electrode, and the solid W electrode and the liquid Cd electrode can be represented by the Nernst equation described as below.

$$E_{Nd} = E_{NdCl_3}^0 + \frac{RT}{3F} \ln \left(\frac{a_{NdCl_3}}{a_{Nd}} \right) - E_{AgCl} \quad (7)$$

$$E_{Nd \text{ in } Cd} = E_{NdCl_3}^0 + \frac{RT}{3F} \ln \left(\frac{a_{NdCl_3}}{a_{Nd \text{ in } Cd}} \right) - E_{AgCl} \quad (8)$$

where E_{Nd} is the potential of Nd at the solid electrode, $E_{Nd \text{ in } Cd}$ is the potential of Nd at the liquid Cd electrode, $E_{NdCl_3}^0$ is the standard electrode potential of $NdCl_3$, E_{AgCl} is the potential of the reference electrode, a_{Nd} is the activity of Nd, a_{NdCl_3} is the activity of $NdCl_3$, $a_{Nd \text{ in } Cd}$ is the activity of Nd in the Nd-Cd phase, R is the gas constant, T is the temperature, F is the Faraday constant, respectively.

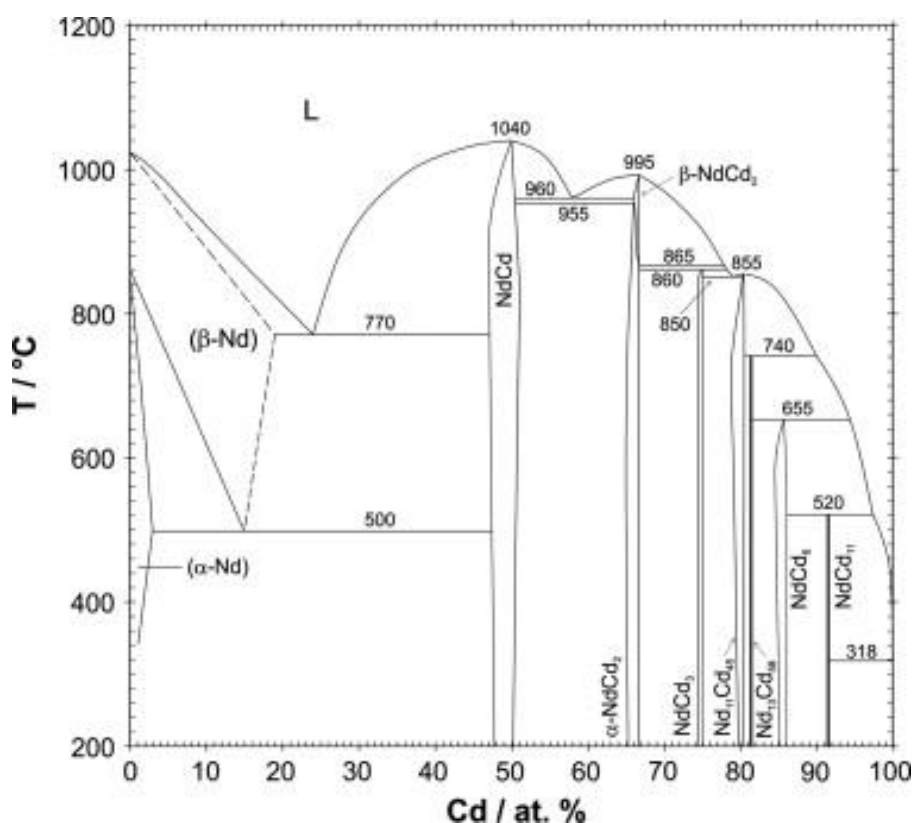


Figure 6. Nd-Cd phase diagram.

Assuming that a_{Nd} is 1, the potential difference between the solid electrode and the liquid Cd electrode is simplified as Equations (7) and (8) shown as below.

$$\Delta E = E_{Nd} - E_{Nd \text{ in } Cd} = \frac{RT}{3F} \ln a_{Nd \text{ in } Cd} \quad (9)$$

The partial Gibbs free energy of Nd using the potential difference can be obtained as shown in Equation (10) below.

$$\Delta G_{Nd} = -3F\Delta E \quad (10)$$

Table 3 summarizes the thermodynamic properties by using the above Equations. Experiments related to this summary are described in detail in the next chapter. Table 3 shows that as the ratio of Cd increases, the potential difference increases, and the activity decreases. Particularly, the Nd-Cd phase diagram shown in Fig. 6 suggests that the compound with the highest ratio of Cd at 500 °C would be NdCd₁₁. If the $a_{Nd \text{ in Cd}}$ at this time is 3.04×10^{-12} , the potential difference (ΔE) is 0.592 V, which is close to 0.540 V obtained from the CV results [37].

Table 3. Thermodynamic properties of Nd for Nd-Cd intermetallic compounds in two-phase coexisting states at 773 K

Two phase region	ΔE_{Nd-Cd} (V vs. Nd ²⁺ /Nd)	ΔG_{Nd} (kJ mol ⁻¹)	$a_{Nd \text{ in Cd}}$
NdCd ₂ and NdCd ₃	0.122±0.007	-35.37±2.10	4.27±0.12×10 ⁻³
NdCd ₃ and Nd ₁₁ Cd ₄₅	0.232±0.007	-67.19±2.25	3.06±0.11×10 ⁻⁵
Nd ₁₁ Cd ₄₅ and Nd ₁₃ Cd ₅₈	0.284±0.006	-82.20±1.98	2.93±0.10×10 ⁻⁶
Nd ₁₃ Cd ₅₈ and NdCd ₆	0.394±0.005	-114.06±1.46	2.01±0.48×10 ⁻⁸
NdCd ₆ and NdCd ₁₁	0.483±0.006	-139.77±1.97	3.78±0.13×10 ⁻¹⁰
NdCd ₁₁ and Cd	0.592±0.011	-171.37±3.34	3.04±0.18×10 ⁻¹²

These results show that the potential difference is due to the decrease in activity induced by the formation of Nd-Cd intermetallic compound.

3.3 Electrochemical reaction of NdCl₃ in LiCl-KCl at Cd-coated W electrode

An experiment was conducted to analyze the formation of Nd-Cd intermetallic compound, by adding a small amount of CdCl₂ to LiCl-KCl-NdCl₃ salt. These experiments have been conducted by numerous researchers, who have reported that useful information on M-Cd intermetallic compound formation can be obtained [10,18,22,38]. Fig. 7 shows the cyclic voltammogram of the LiCl-KCl-1 wt% NdCl₃-0.2 wt% CdCl₂ salt measured with a W electrode at a scan rate of 0.1 V/s. Unlike Fig. 1, the results show many peaks in addition to the oxidation-reduction peaks of Nd, indicating that many Nd_xCd_y intermetallic compounds are being formed and decomposed. Thus, when the potential increases in the negative direction, Cd begins to be reduced at approximately -0.6 V, and the surface of the W electrode is coated with Cd. When the potential increases further in the negative direction, Nd starts to be reduced together with the Cd to form an alloy, which results in a numerous reduction peaks. Conversely, when the potential increases in the positive direction, the first oxidation peak appears at -2.038 V, which suggests that Nd is oxidized to Nd²⁺ ion. Subsequently, during the

dissociation of Nd in the Nd_xCd_y alloy into LiCl-KCl salt, six oxidation peaks appear sequentially and Cd is oxidized at approximately -0.5 V.

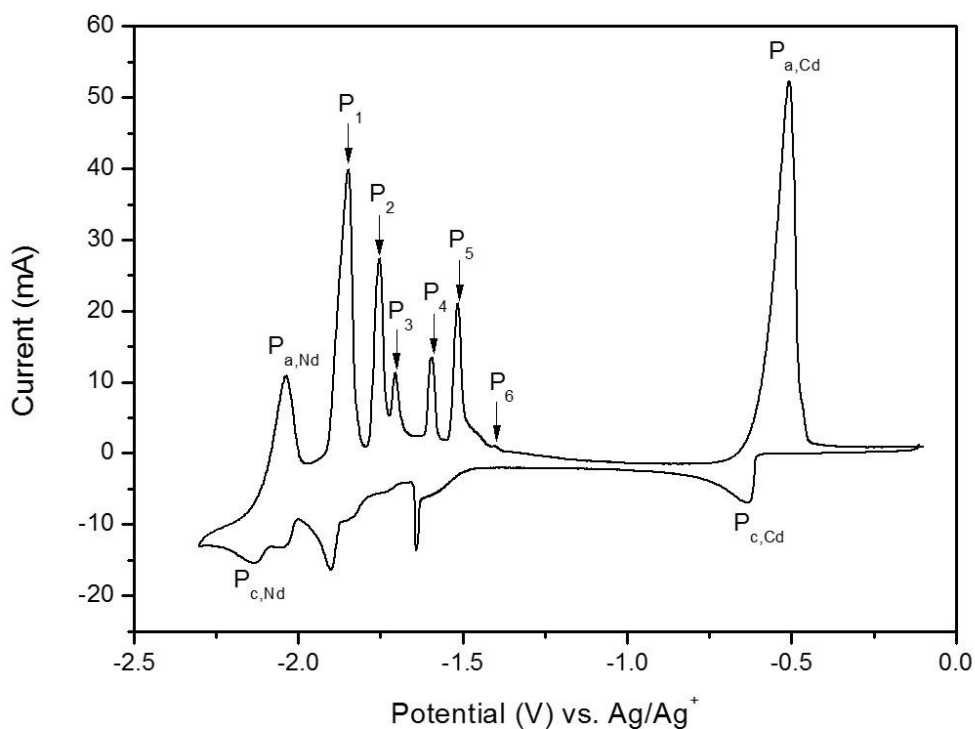


Figure 7. Cyclic voltammogram of LiCl-KCl-NdCl₃-CdCl₂ at W electrode with the scan rate of 0.1 V/s. Temperature: 773 K; Concentration of NdCl₃ and CdCl₂: 1 wt% and 0.2 wt%; Electrode area: 0.256 cm²

These peaks are more clearly distinguished in the oxidation direction than in the reduction direction. The reduction peak due to the Nd(III)/Nd(II) reaction shown in Fig. 1 are difficult to distinguish by the CV as in the other peaks, and its oxidation peak have the potential similar to that of P₁, and thus, peaks are overlapped, which are indistinguishable. However, since the current value of the Nd(III)/Nd(II) peak is negligibly small as compared with the value from the CV curve without CdCl₂, the oxidation reaction of the Nd_xCd_y intermetallic compound is dominant at the corresponding potential.

The chemical composition of Nd_xCd_y can be estimated by comparing the number of cumulative coulombs in P_{a,Cd}, P_{a,Nd}, P₁, P₂, P₃, P₄, P₅, and P₆ because Cd and Nd are reduced together at a potential lower than -0.5 V in the cathodic sweep, while Nd is oxidized alone until the potential reaches around -0.5 V in the anodic sweep [22]. Since the accumulated charge amount from P_{a,Nd} to P₆ means the amount of dissociated Nd, it is possible to calculate the ratio of Nd/Cd at each peak through comparison with P_{a,Cd}. Accordingly, the ratio of Nd/Cd from P₁ to P₆ is 0.589, 0.371, 0.279, 0.235, 0.145, and 0.085, respectively.

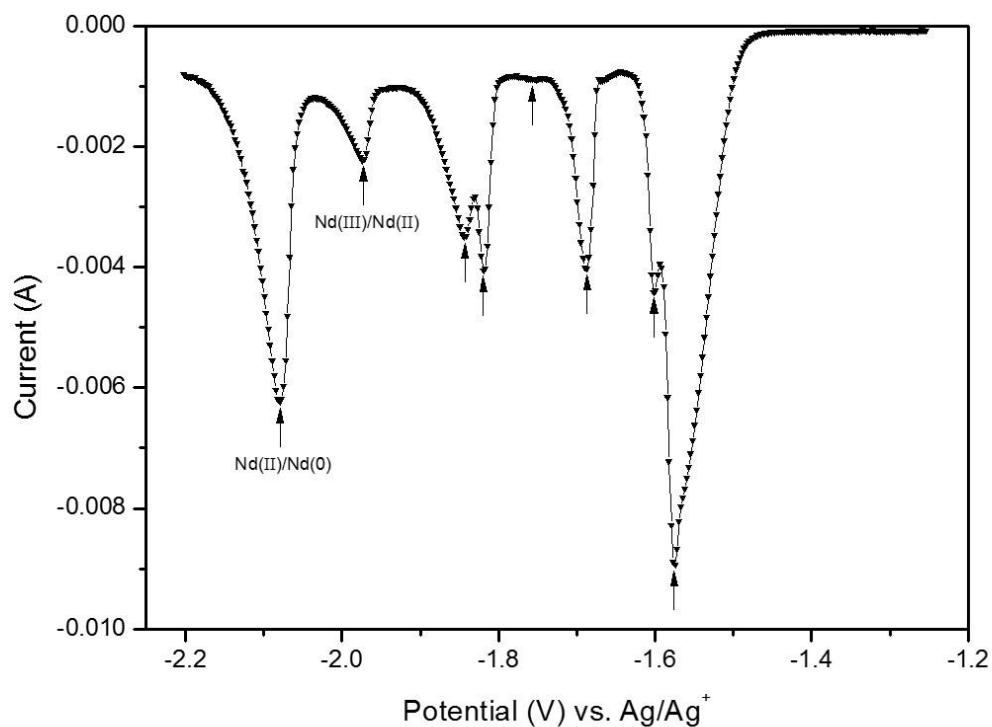


Figure 8. Square wave voltammogram of LiCl-KCl-NdCl₃-CdCl₂ at W electrode. Temperature: 773 K; Concentration of NdCl₃ and CdCl₂: 1 wt% and 0.1 wt%; Electrode area: 0.256 cm²; Frequency: 8 Hz; Amplitude of pulse: 5 mV.

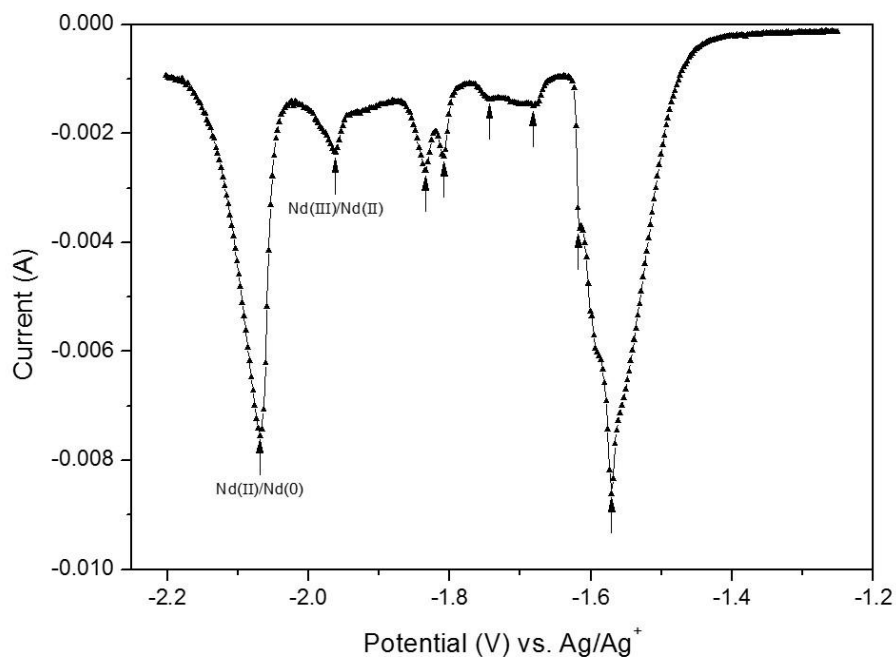


Figure 9. Differential pulse voltammogram of LiCl-KCl-NdCl₃-CdCl₂ at W electrode. Temperature: 773 K; Concentration of NdCl₃ and CdCl₂: 1 wt% and 0.1 wt%; Electrode area: 0.256 cm²; Amplitude of pulse: 5 mV.

According to the Nd-Cd phase diagram, there are six Nd_xCd_y compounds such as NdCd_2 , NdCd_3 , $\text{Nd}_{11}\text{Cd}_{45}$, $\text{Nd}_{13}\text{Cd}_{58}$, NdCd_6 , NdCd_{11} when the concentration of Cd is 50 % or more at 500 °C (Fig. 6) [37]. P_1 , P_2 , P_3 , P_4 , P_5 , and P_6 peaks correspond to the above-mentioned compounds, respectively, since the ratio of Nd/Cd to the respective compositions is theoretically 0.5, 0.333, 0.244, 0.224, 0.167 and 0.091.

The SWV and DPV, which belong to the pulse voltammetry techniques, were performed to identify the reduction peak. The SWV and DPV are widely used in the analysis of electroactive materials because the SWV and DPV show more specific electrode responses according to the potential due to the low influence by charging current [39,40]. Figs. 8 and 9 show the results of the SWV and DPV measured in $\text{LiCl-KCl-1 wt\% NdCl}_3\text{-0.1 wt\% CdCl}_2$, respectively. Furthermore, as shown in Figs. 8 and 9, six reduction peaks other than the Nd(III)/Nd(II) and Nd(II)/Nd(0) peaks are observed, which means that six Nd_xCd_y intermetallic compounds are formed. Particularly, the potentials of the first peak in the negative direction are -1.574 V and -1.571 V, respectively. Those values are close to -1.568 V, which is the reduction peak potential using the liquid Cd electrode. Thus, the results indicate that the formation of NdCd_{11} occurs in the liquid Cd electrode because the use of the liquid Cd electrode prevents other intermetallic compounds than NdCd_{11} from forming due to the extremely higher Cd concentration than that of Nd on the electrode surface. A study by Vandarkuzhali et al. conducted an experiment in which a large amount of Cd was electrodeposited on a W electrode, followed by electrodeposition of NdCl_3 , and further reported that the precipitated Nd-Cd intermetallic compound was NdCd_{11} [25]. These results suggest that the experiment using Cd-coated electrode is a useful method for characterizing liquid Cd electrode reaction.

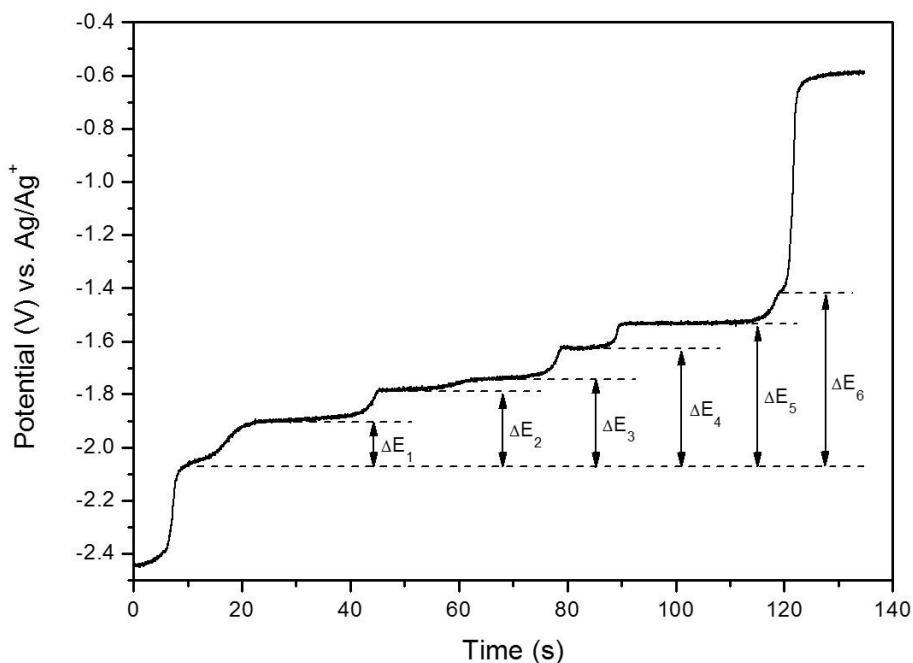


Figure 10. Chronopotentiogram of $\text{LiCl-KCl-NdCl}_3\text{-CdCl}_2$ at W electrode. Temperature: 773 K; Concentration of NdCl_3 and CdCl_2 : 1 wt% and 0.1 wt%; Applied current: 1 μA .

The CP experiment was conducted to analyze the thermodynamic properties of Nd-Cd intermetallic compounds such as Gibbs free energy and activity. The experiment was performed according to the following procedure. First, a current of -20 mA was applied to LiCl-KCl-1 wt% NdCl₃-0.1 wt% CdCl₂ salt for 30 seconds to deposit Cd and Nd simultaneously on the surface of the solid W electrode. Subsequently, a current of 1 μA was applied, and the changes in potential over time were observed. Nd and Cd dissociate into LiCl-KCl salt because of the positive current flow. Fig. 10 shows that the reactions occur at approximately -2.0 V and -0.6 V, respectively. Also, there are six potential plateaus due to the dissociation of Nd in the Cd film into the salt, and the potential increases in the positive direction and the plateaus are formed sequentially. Many researchers have reported that this potential plateau in the CP experiment means is a two-phase region [21,33,41-44]. According to the studies, when the compounds of the two different compositions coexist on the surface of the electrode, the activity of the metal element is maintained constant by the equilibrium until one compound completely changes to another compound, and thus, the electro motive force (EMF) remains constant [42].

Thus, the two-phase region corresponding to the potential plateaus in this experiment are NdCd₂-NdCd₃, NdCd₃-Nd₁₁Cd₄₅, Nd₁₁Cd₄₅-Nd₁₃Cd₅₈, Nd₁₃Cd₅₈-NdCd₆, NdCd₆-NdCd₁₁, NdCd₁₁-Cd, respectively. Accordingly, the potential difference between Nd(III) Nd(II) and plateau corresponds to the EMF of the two-phase region. The activity and Gibbs free energy of Nd in the binary phase can be calculated by using Equations (9) and (10) described in 3.2. To ensure reproducibility, the CP experiments were performed several times under the same conditions, and Table 3 summarizes the calculation results.

Using the potential difference, the standard Gibbs free energies of formation for the intermetallic compounds can be obtained by using the following Equations [18,33].

$$\Delta G_f^0(\text{NdCd}_{11}) = -3F\Delta E_6 \quad (11)$$

$$\Delta G_f^0(\text{NdCd}_{x_2}) = -3F \int_{x_2}^{x_1} \Delta E(x) dx + \Delta G_f^0(\text{NdCd}_{x_1}) \quad (12)$$

where ΔG_f^0 is the standard Gibbs free energy of formation for the Nd-Cd intermetallic compound, x_1 , and x_2 are the stoichiometric coefficients of Cd ($x_1, x_2 = 11, 6, 58/13, 45/11, 3, 2, x_1 > x_2$).

Table 4 summarizes equations and the results to calculate the Gibbs free energy of formation for each Nd-Cd compound. There is no reported thermodynamic data for any meaningful comparison. Although the study by Vandarkuzhali et al. analyzed the thermodynamic properties of Nd-Cd compounds by using the CP, only the result of NdCd₁₁ were obtained [25]. That study reported that α_{Nd} in Cd and $\Delta G_{f,\text{NdCd}_{11}}^0$ were 6.31×10^{-11} and -150.8 kJ/mol, respectively, which were slightly higher than those in this study. The results suggest that the slight difference of $\Delta E_{\text{Nd-Cd}}$ (approximately 0.06 V) between the two studies occurred due to the different experimental conditions. However, the trends in the thermodynamic properties are highly consistent in the results of both studies.

Table 4. Gibbs free energies of formation for Nd-Cd intermetallic compounds at 773 K

Reaction of alloy formation	Equation	ΔG_f^0 (kJ mol ⁻¹)
$\text{Nd} + 2\text{Cd} \rightarrow \text{NdCd}_2$	$\Delta G_{f,\text{NdCd}_2}^0 = \frac{1}{3}[2\Delta G_{f,\text{NdCd}_3}^0 - 3F\Delta E_1]$	-92.59±2.88
$\text{Nd} + 3\text{Cd} \rightarrow \text{NdCd}_3$	$\Delta G_{f,\text{NdCd}_3}^0 = \frac{4}{15}\left[\frac{11}{4}\Delta G_{f,\text{NdCd}_{45/11}}^0 - 3F\Delta E_2\right]$	-120.18±2.85
$\text{Nd} + \frac{45}{11}\text{Cd} \rightarrow \text{NdCd}_{45/11}$	$\Delta G_{f,\text{NdCd}_{45/11}}^0 = \frac{53}{638}\left[\frac{585}{53}\Delta G_{f,\text{NdCd}_{58/13}}^0 - 3F\Delta E_3\right]$	-141.03±3.34
$\text{Nd} + \frac{58}{13}\text{Cd} \rightarrow \text{NdCd}_{58/13}$	$\Delta G_{f,\text{NdCd}_{58/13}}^0 = \frac{20}{78}\left[\frac{58}{20}\Delta G_{f,\text{NdCd}_6}^0 - 3F\Delta E_4\right]$	-144.99±2.67
$\text{Nd} + 6\text{Cd} \rightarrow \text{NdCd}_6$	$\Delta G_{f,\text{NdCd}_6}^0 = \frac{5}{11}\left[\frac{6}{5}\Delta G_{f,\text{NdCd}_{11}}^0 - 3F\Delta E_5\right]$	-157.86±2.11
$\text{Nd} + 11\text{Cd} \rightarrow \text{NdCd}_{11}$	$\Delta G_{f,\text{NdCd}_{11}}^0 = -3F\Delta E_6$	-171.37±3.34

4. CONCLUSION

This study investigated the Nd(III)/Nd(0) electrode reaction in the LiCl-KCl-NdCl₃ molten salt by using a solid W electrode and a liquid Cd electrode. The results of CV measurement showed that the Nd(III)/Nd(0) reaction has an intermediate step of forming Nd(II) ion in the solid W electrode, resulting in two steps in total. On the other hand, a pair of redox reaction occurred at the liquid Cd electrode, and the reduction peak potential of the liquid Cd electrode was approximately 0.54 V higher than that of the solid W electrode. This potential difference occurs due to the formation of an Nd-Cd intermetallic compound where reduced Nd reacts with Cd of the liquid electrode, and the activity of Nd becomes smaller due to the formation of an intermetallic compound. The experimental results using CdCl₂ showed that the formation of Nd-Cd intermetallic compound was confirmed by the methods such as CV and CP. Particularly, when Cd is the main component, a reaction forming NdCd₁₁ occurs, which could occur in the liquid Cd electrode. The CP experiment results were used to calculate the Gibbs free energy and activity of Nd-Cd intermetallic compounds, and the results are similar to those of other researchers.

ACKNOWLEDGEMENTS

This work was supported by a National Research Foundation of Korea (NRF) grant funded by the Korean government (MSIP) (No.2017M2A8A5015079).

References

1. H.S. Lee, J.M. Hur and D.H. Ahn et al., Korea Atomic Energy Research Institute (KAERI) report, Report No. KAERI/RR-3400/2011, Republic of Korea.
2. J.P. Ackerman, *Ind. Eng. Chem. Res.*, 30 (1991) 141.
3. J.L. Willit, W.E. Miller and J.E. Battles, *J. Nucl. Mater.*, 195 (1992) 229.

4. T. Inoue and L. Koch, *Nucl. Eng. Technol.*, 40 (2008) 183.
5. S.X. Li, S.D. Herrmann, K.M. Goff and M.F. Simpson, *Nucl. Technol.*, 165 (2009) 190.
6. T. Kato, T. Inoue, T. Iwai and Y. Arai, *J. Nucl. Mater.*, 357 (2006) 105.
7. T.J. Kim, A. Uehara, T. Nagai, T. Fujii and H. Yamana, *J. Nucl. Mater.*, 409 (2011) 188.
8. K. Uozumi, M. Iizuka, T. Kato, T. Inoue, O. Shirai, T. Iwai and Y. Arai, *J. Nucl. Mater.*, 325 (2004) 34.
9. A.F. Laplace, J. Lacquement, J.L. Willit, R.A. Finch, G.A. Fletcher and M.A. Williamson, *Nucl. Technol.*, 163 (2008) 366.
10. S.H. Kim, S.W. Paek, T.J. Kim, D.Y. Park and D.H. Ahn, *Electrochim. Acta*, 85 (2012) 332.
11. G.Y. Kim, T.J. Kim, D.H. Ahn and S.W. Paek, *Asian J. Chem.*, 25 (2013) 7527.
12. S.A. Kuznetsov and M. Gaune-Escard, *J. Electroanal. Chem.*, 595 (2006) 11.
13. Y. Castrillejo, M.R. Bermejo, E. Barrado, A.M. Martinez and P. Diaz Arocas, *J. Electroanal. Chem.*, 545 (2003) 141.
14. P. Masset, R.J.M. Konings, R. Malmbeck, J. Serp and J.P. Glatz, *J. Nucl. Mater.*, 344 (2005) 173.
15. G. Bourges, D. Lambertin, S. Rochefort, S. Delpech and G. Picard, *J. Alloys Compd.*, 444 (2007) 404.
16. S.A. Kuznetsov and M. Gaune-Escard, *J. Nucl. Mater.*, 389 (2009) 108.
17. S. Kobayashi, K. Kobayashi, T. Nohira, R. Hagiwara, T. Oishi and H. Konishi, *J. Electrochim. Soc.*, 158 (2011) 142.
18. Y. Castrillejo, M.R. Bermejo, P. Diaz Arocas, A.M. Martinez and E. Barrado, *J. Electroanal. Chem.*, 579 (2005) 343.
19. G. De Cordoba, A. Laplace, O. Conocar, J. Lacquement and C. Caravaca, *Electrochim. Acta*, 54 (2008) 280.
20. O. Shirai, K. Uozumi, T. Iwai and Y. Arai, *Anal. Sci.*, 17 (2001) 159.
21. O. Shirai, M. Iizuka, T. Iwai, Y. Suzuki and Y. Arai, *J. Electroanal. Chem.*, 490 (2000) 31.
22. O. Shirai, A. Uehara, T. Fujii and H. Yamada, *J. Nucl. Mater.*, 344 (2005) 142.
23. D.S. Yoon, S. Phongikaroon and J. Zhang, *J. Electrochem. Soc.*, 163 (2016) E97.
24. Y. Castrillejo, M.R. Bermejo, P. Diaz Arocas, A.M. Martinez and E. Barrado, *J. Electroanal. Chem.*, 575 (2005) 61.
25. S. Vandarkuzhali, Manish Chandra, Suddhasattwa Ghosh, Nibedita Samanta, S. Nedumaran, B. Prabhakara Reddy and K. Nagarajan, *Electrochim. Acta*, 145 (2014) 86.
26. K. Fukasawa, A. Uehara, T. Nagai, T. Fujii and H. Yamana, *J. Alloys Compd.*, 509 (2011) 5112.
27. S.A. Kuznetsov and M. Gaune-Escard, *Electrochim. Acta*, 46 (2001) 1101.
28. A. Novoselova and V. Smolenski, *Electrochim. Acta*, 87 (2013) 657.
29. A.J. Bard, L.R. Faulkner, *Electrochemical Methods: Fundamentals and Applications*, 2nd ed., John Wiley & Sons, Inc., (2001) Hoboken, USA.
30. B. Prabhakara Reddy, S. Vandarjuzhali, T. Subramanian and P. Venkatesh, *Electrochim. Acta*, 49 (2004) 2471.
31. T. Store, G.M. Haarberg and R. Tunold, *J. Appl. Electrochem.*, 30 (2000) 1351.
32. J.P. Glatz, R. Malmbeck, C. Pernel, C. Scheppler and J. Serp, PYROREP Contract No. FIKW-CT-2000-00049, Project No. FIS5-1999-00199.
33. Y. Castrillejo, R. Bermejo, R. Fernandez, E. Barrado and P. Diaz Arocas, *J. Nucl. Mater.*, 360 (2007) 32.
34. T. Koyama, T.R. Johnson and D.F. Fischer, *J. Alloy. Compd.*, 189 (1992) 37.
35. M. Kurata, Y. Sakamura and T. Matsui, *J. Alloy. Compd.*, 234 (1996) 83.
36. M. Sakata, M. Kurata, T. Hijikata and T. Inoue, *J. Nucl. Mater.*, 185 (1991) 56.
37. B. Skolyszewska-Kuhberger, T.L. Reichmann and H. Ipsen, *J. Alloy. Compd.*, 606 (2014) 242.
38. H. Shibata, H. Hayashi, M. Akabori, Y. Arai and M. Kurata, *J. Phys. Chem. Solids*, 75 (2014) 972.
39. J.L. Lyon and K.J. Stevenson, *Anal. Chem.* 78 (2006) 8518.
40. F.A. Bertolino, A.A.J. Torriero, E. Salinas, R. Olsina, L.D. Martinez and J. Raba, *Anal. Chim. Acta*

572 (2006) 32.

41. O. Shirai, M. Iizuka, T. Iwai and Y. Arai, *J. Appl. Electrochem.*, 31 (2001) 1055.

42. H. Konishi, T. Nohira and Y. Ito, *J. Electrochem. Soc.*, 148 (2001) C506.

43. M.R. Bermejo, J. Gomez, J. Medina, A.M. Martinez and Y. Castrillejo, *J. Electroanal. Chem.*, 588 (2006) 253.

44. P. Taxil and J. Mahenc, *J. Appl. Electrochem.*, 17 (1987) 261.

© 2018 The Authors. Published by ESG (www.electrochemsci.org). This article is an open access article distributed under the terms and conditions of the Creative Commons Attribution license (<http://creativecommons.org/licenses/by/4.0/>).